Reducing the Effects of Noise in Image Reconstruction

Rick Archibald[1] **and A. Gelb**[1]

Fourier spectral methods have proven to be powerful tools that are frequently employed in image reconstruction. However, since images can be typically viewed as piecewise smooth functions, the Gibbs phenomenon often hinders accurate reconstruction. Recently, numerical edge detection and reconstruction methods have been developed that effectively reduce the Gibbs oscillations while maintaining high resolution accuracy at the edges. While the Gibbs phenomenon is a standard obstacle for the recovery of all piecewise smooth functions, in many image reconstruction problems there is the additional impediment of random noise existing within the spectral data. This paper addresses the issue of noise in image reconstruction and its effects on the ability to locate the edges and recover the image. The resulting numerical method not only recovers piecewise smooth functions with very high accuracy, but it is also robust in the presence of noise.

1. INTRODUCTION

High quality image reconstruction from Fourier spectral data is an important aspect in many scientific disciplines. The ability to visualize complicated structures is an essential diagnostic tool that impacts discoveries and technological advances in fields such as astrophysics, computer science, medicine, and biology. Due to their very accurate results and ease of implementation, Fourier spectral methods have proven to be powerful tools and are frequently employed in image reconstruction. These images can typically be viewed as piecewise smooth functions, giving rise to the infamous Gibbs phenomenon that both produces spurious oscillations at the jump discontinuities as well as drastically reduces the overall convergence rate. The effectiveness of image reconstruction as a diagonostic tool is hence

---

[1] Department of Mathematics, Arizona State University, Tempe, Arizona 85287-1804. E-mail: {rick;ag}@math.la.asu.edu

severely limited, since it is unclear whether actual features or noisy artifacts of the image are being visualized. Recent work has been instrumental in developing methods that effectively combat Gibbs oscillations without causing undesirable blurring at the feature edges of the image.

Another important component of image reconstruction is edge detection. All high resolution reconstruction methods require a priori knowledge of the jump discontinuity locations to determine intervals of smoothness in which the function can be reconstructed. Once the edges of the image are located, Gibbs reduction techniques can be successfully applied.

While the Gibbs phenomenon is a standard obstacle for all piecewise smooth function reconstructions, in many applications there is the additional impediment of random noise existing within the spectral data. Typically this noise is difficult to quantify and can not be systematically removed. In this paper we address the issue of noise in image reconstruction and its effects on the ability to locate the edges and recover the image. The resulting numerical method for edge detection and reconstruction not only recovers piecewise smooth functions with very high accuracy, but is also robust in the presence of noise. The paper is organized as follows: In Section 2 we describe the edge detection method developed in [7] and [8] and further developed in [2]. We also briefly review the Gegenbauer reconstruction method [10] for piecewise smooth functions. In Section 3 a modification to the edge detection procedure is introduced to combat the effects of noise. Numerical examples for the edge detection and Gegenbauer reconstruction of images with noise are provided.

2. HIGH RESOLUTION IMAGE RECONSTRUCTION

2.1. Edge Detection

As mentioned in the introduction, all high resolution reconstruction methods for piecewise smooth functions require a priori knowledge of the locations of the discontinuities. Additionally, the locations and amplitudes of jump discontinuities provide valuable information in many scientific applications. For instance, in magnetic resonance imaging (MRI), the locations and amplitudes of edges are necessary in determining tissue type and density [12]. The concentration method, developed in [7] and [8], and later modified in [2], successfully detects edges and their corresponding heights in a robust and simple manner. Furthermore, as will be discussed in Section 3, the method is readily adaptable to data containing noise, a crucial development allowing the method to be viable for practical applications.

To briefly summarize the concentration method, let us define a jump function of a piecewise smooth and periodic function $f(x)$ as $[f](x) := f(x+) - f(x-)$, where $f(x\pm)$ are the right and left side limits of the

function at x. When the continuous Fourier coefficients $\hat{f}_k$ are known, the concentration method is equivalent to solving [7]

$$S_N^\sigma[f](x) = i\pi \sum_{k=-N}^{N} \text{sgn}(k)\, \sigma\left(\frac{|k|}{N}\right) \hat{f}_k e^{ik\pi x} \tag{2.1}$$

It was shown in [7] that if the concentration factors $\sigma(\xi)$ satisfy

$$\frac{\sigma(\xi)}{\xi} \in C^2[0,1] \qquad \text{and} \qquad \int_0^1 \frac{\sigma(\xi)}{\xi}\, d\xi = 1 \tag{2.2}$$

then the following concentration property holds:

$$S_N^\sigma[f](x) \to [f](x), \qquad \text{as} \quad N \to \infty \tag{2.3}$$

The analogous case for the discrete Fourier coefficients, $\tilde{f}_k$, implemented as

$$T_N^\tau[f](x) := i\pi \sum_{k=-N}^{N} \text{sgn}(k)\, \tau\left(\frac{|k|}{N}\right) \tilde{f}_k e^{ik\pi x}, \qquad \tau(\xi) = \sigma(\xi)\frac{2\sin\left(\dfrac{\xi\pi}{2}\right)}{\xi\pi} \tag{2.4}$$

admits a concentration property akin to (2.3) ensuring convergence of (2.4) to $[f](x)$. Several examples of admissible concentration factors are discussed in [7]. One particularly effective factor is the exponential concentration factor,

$$\sigma_e(\xi) = \text{Const} \cdot \xi e^{\frac{1}{\alpha\xi(\xi-1)}}, \qquad \tau_e(\xi) = \sigma_e(\xi)\frac{2\sin\left(\dfrac{\xi\pi}{2}\right)}{\xi\pi} \tag{2.5}$$

where $\text{Const} = \int_\epsilon^{1-\epsilon} \exp(\frac{-1}{\alpha\eta(\eta-1)})\, d\eta$ for $\epsilon \sim \mathcal{O}(\frac{1}{N})$ with typical $\alpha \approx 6$.

Although the concentration method tends to the singular support of the function, it must be further enhanced to pinpoint the jump discontinuity locations. This has been achieved in [8] by separating the vanishing scales in the smooth regions from the $\mathcal{O}(1)$ scales in the neighborhoods of the jump discontinuities. Specifically, if $\{x_j^*\}_{j=1}^M$ denote the locations of the jump discontinuities of $f(x)$, then for admissible concentration factors in (2.4), the separation of scales is enhanced by computing

$$E := N^{q/2}(T_N^\tau[f](x))^q \to \begin{cases} N^{q/2}([f](x_j^*))^q, & \text{if} \quad x = x_j^*, \\ \mathcal{O}(N^{-q/2}), & \text{if} \quad x \neq x_j^* \end{cases}$$

leading to the enhanced concentration method,

$$E_N(T_N^\tau[f](x)) = \begin{cases} T_N^\tau[f](x), & \text{if} \quad |E| > J_{\text{crit}}, \\ 0, & \text{if} \quad |E| < J_{\text{crit}}, \end{cases} \tag{2.6}$$

Here J_{crit} is an $\mathcal{O}(1)$ global threshold parameter signifying the minimal amplitude for the jump discontinuity not to be negligible. The jump location is the point corresponding to the largest value in an $\mathcal{O}(\epsilon(N))$ neighborhood.

The nonlinear enhancement procedure (2.6) works well enough for images that have edges far enough apart, e.g., more than $\mathcal{O}(\epsilon(N))$, but the oscillations resulting from the concentration method (2.4) in the neighborhoods of discontinuities make it very difficult to locate discontinuities that are close together [2]. This issue is of upmost importance in many scientific applications, since there is not enough resolution to guarantee that the discontinuities are located far enough apart. The concentration method has since been further developed [2] in order to successfully locate edges that are very close together. The approach applies the simple idea of subtracting out a saw tooth function from a piecewise smooth function to create an analytic function, an idea currently utilized in several reconstruction techniques [4–6]. Specifically, consider $f(x)$ to be a periodic piecewise smooth function. Then

$$h(x) := f(x) - \sum_{i=1}^{M} \frac{a_i}{2} g(x; x_i^*)$$

is a periodic smooth function, where $g(x; x_i^*)$ is the saw tooth function

$$g(x; x_i^*) = \begin{cases} -(1+x) & \text{if} \quad -1 \leqslant x \leqslant x_i^*, \\ 1-x & \text{if} \quad x_i^* < x \leqslant 1 \end{cases}$$

Here $x = \{x_i^*\}_{i=1}^{M}$ are the jump locations with corresponding jump values $[f](x_i^*) = a_i$. Since $[h](x) = 0$, the concentration property (2.3) establishes the minimization problem,

$$\min_{M, a_i, x_i^*} \max_x |T_N^\tau[h](x)| := \min_{M, a_i, x_i^*} \max_x \left| T_N^\tau[f](x) - \sum_{i=1}^{M} \frac{a_i}{2} T_N^\tau[g](x; x_i^*) \right| \tag{2.7}$$

to yield the size and positions of the jump discontinuities. The enhancement results from (2.6) serve as good initialization parameters. For higher dimensional images, the procedure is performed dimension by dimension. Algorithmic details can be found in [2].

We note that although knowing the heights of the jump discontinuities is not necessary to reconstruct piecewise smooth functions, it is of vital importance in many scientific applications. Many images have very complicated structure where various features are seen across only a few pixels. In places where the image lacks resolution, high order reconstruction is replaced by connecting information from one edge to another, making knowledge of the correct jump heights imperative.

2.2. Gegenbauer Reconstruction

Much research has been devoted to developing reconstruction techniques for piecewise smooth functions. The Gegenbauer reconstruction method, developed in [11] and extended in a series of articles listed in [10], recovers piecewise smooth functions with spectral accuracy *up to* the edges in each smooth interval. It can therefore be used to completely eliminate the Gibbs oscillations without compromising high resolution at the edges. A detailed analysis of the Gegenbauer reconstruction method can be found in [10].

Let $f(x)$ be a piecewise smooth function in $[-1, 1]$ that is analytic in a sub-interval $[a, b]$. The truncated (pseudo-) spectral Fourier expansion on $[a, b]$, given by

$$f_N(x) = \sum_{k=-N}^{N} \hat{f}_k e^{ik\pi x} \tag{2.8}$$

can be used to approximate the Gegenbauer coefficients as

$$\hat{g}_{l,\epsilon}^{\lambda} = \frac{1}{h_l^{\lambda}} \int_{-1}^{1} (1-\eta^2)^{\lambda-\frac{1}{2}} C_l^{\lambda}(\eta) \, f_N(x(\eta)) \, d\eta \tag{2.9}$$

where $h_l^{\lambda} = \sqrt{\pi} \, C_l^{\lambda}(1) \frac{\Gamma(\lambda+1/2)}{\Gamma(l)(l+\lambda)}$ and the local variable $\eta \in [-1, 1]$ is defined such that $x(\eta) = \epsilon\eta + \delta$ with $\epsilon = \frac{b-a}{2}$ and $\delta = \frac{b+a}{2}$. The Gegenbauer partial sum approximation, based on the orthogonal Gegenbauer polynomials $C_l^{\lambda}(\eta)$, is computed as

$$g_m^{\lambda}(x(\eta)) = \sum_{l=0}^{m} \hat{g}_{l,\epsilon}^{\lambda} C_l^{\lambda}(\eta) \tag{2.10}$$

It was shown in [10] that (2.10) provides an exponentially convergent approximation to $f(x)$ in $[a, b]$ in the maximum norm provided that $\lambda, m \sim \epsilon N$ [10]. Hence the poorly performing Fourier approximation (2.8) is turned into an exponentially converging approximation for a piecewise smooth function $f(x)$ in $[-1, 1]$ by applying the Gegenbauer reconstruction method, (2.9) and (2.10), in each smooth sub-interval $[a, b]$ and then "gluing" the results together. The boundaries of each sub-interval are first determined by the edge detection procedure described in Section 2.1.

Although computation of (2.9) appears somewhat formidable, exploitation of the relationship [3]

$$\hat{g}_{l,\epsilon}^{\lambda} = \delta_{0l}\hat{f}_0 + \Gamma(\lambda) \, i^l(l+\lambda) \sum_{0 < |k| \leqslant N} J_{l+\lambda}(\pi k\epsilon) \left(\frac{2}{\pi k\epsilon}\right)^{\lambda} \hat{f}_k e^{ik\pi\delta} \tag{2.11}$$

allows employment of the FFT in the calculation of the Gegenbauer coefficients (2.9).

(a)   (b)
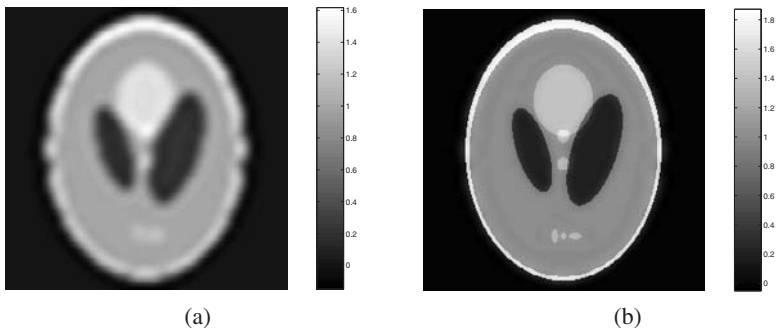
Fig. 1. (a) Filtered Fourier reconstruction of the Shepp Logan brain phantom with exponential filter of order $p = 4$ and (b) the Gegenbauer reconstruction with $m = \lambda \approx \frac{\epsilon N}{8}$ on 128×128 data pixels.

To close this section, we use Fig. 1 to illustrate the efficacy of the edge detection procedure described in Section 2.1 and the Gegenbauer reconstruction method for the Shepp Logan phantom brain image (see, e.g., [9] and [12].) Figure 1(a) shows the standard filtered Fourier approximations of the Shepp Logan image, where it is evident that the filtered Fourier reconstruction produces undesirable blurring at the edges. The results of the edge detection procedure, comprised of (2.4), (2.6), and (2.7), are used to determine each smooth sub-interval. This enables the application of the Gegenbauer reconstruction method which yields the high resolution reconstruction of the Shepp Logan phantom image displayed in Fig. 1(b).

3. NOISE CHARACTERISTICS IN THE DATA DOMAIN

In the development and testing of image reconstruction techniques, it is common to assume certain characteristics about the signal, namely that the signal can be modeled by a stochastic process. Described below is the study of noise from a random variable perspective, [12], which will be used to develop techniques in noise reduction. Suppose that a signal (Fourier coefficient) can be modeled as the correct spectral data plus the corruption in the spectral data,

$$\bar{f}_k = \hat{f}_k + \hat{\xi}_k \tag{3.1}$$

We further assume that $\hat{\xi}_k$ is a complex additive noise coming from an ergodic, stationary, uncorrelated, white noise process with zero mean $E\{\hat{\xi}_k\} = 0$, and standard of deviation $\hat{\sigma}_{\xi} > 0$ as defined by the variance, $\mathrm{Var}(\hat{\xi}_k) := E\{[\hat{\xi}_k - E\{\hat{\xi}_k\}] \cdot [\hat{\xi}_k - E\{\hat{\xi}_k\}]^*\} = \hat{\sigma}_{\xi}^2$. The image noise is given by

$$\xi_N(x) = \sum_{k=-N}^{N} \hat{\xi}_k e^{i\pi k x} \tag{3.2}$$

Several properties are derived directly from (3.2), given in [12] as

1. The mean of the image noise is zero, $E\{\xi_N(x)\} = 0$,
2. The variance of the image noise is given by $\sigma_N^2 = (2N+1)\,\hat{\sigma}_{\hat{\xi}}^2$,
3. The image noise is uncorrelated from data point to data point, $E\{\xi_N(x)\,\xi_N(y)\} = 0$ for $x \neq y$.

The Fourier reconstructed image with noise can now be written as

$$I_N(x) = \sum_{k=-N}^{N} \bar{f}_k e^{ik\pi x} = \sum_{k=-N}^{N} (\hat{f}_k + \hat{\xi}_k)\, e^{ik\pi x} = f_N(x) + \xi_N(x)$$

implying that the image will be the sum of the Fourier reconstruction of the correct spectral data and the image noise (3.2). The calculation of the expectation of the reconstructed image,

$$E\{I_N(x)\} = E\left\{ \sum_{k=-N}^{N} (\hat{f}_k + \hat{\xi}_k)\, e^{ik\pi x} \right\} = E\{f_N(x)\} + E\{\xi_N(x)\} = f_N(x)$$

demonstrates that the average value of the reconstructed image is the standard Fourier reconstruction of the image without noise. Hence the Fourier reconstruction of the image is an unbiased estimator of the Fourier reconstruction of uncorrupted data. The variance is computed as

$$
\begin{aligned}
\mathrm{Var}(I_N(x)) &= E\left\{ \left[\sum_{k=-N}^{N} (\hat{f}_k + \hat{\xi}_k)\, e^{ik\pi x} - E\{I_N(x)\} \right] \right.\\
&\qquad \left. \cdot \left[\sum_{j=-N}^{N} (\hat{f}_j + \hat{\xi}_j)\, e^{ij\pi x} - E\{I_N(x)\} \right]^* \right\}\\
&= E\left\{ \left[\sum_{k=-N}^{N} \hat{\xi}_k e^{ik\pi x} \right] \cdot \left[\sum_{j=-N}^{N} \hat{\xi}_j e^{ij\pi x} \right]^* \right\}\\
&= \sum_{k=-N}^{N} \sum_{j=-N}^{N} E\{\hat{\xi}_k \hat{\xi}_j^*\}\, e^{ik\pi x} e^{ij\pi x}\\
&= \sum_{k=-N}^{N} E\{\hat{\xi}_k \hat{\xi}_k^*\}\, e^{2ik\pi x} = (2N+1)\,\hat{\sigma}_{\hat{\xi}}^2 = \sigma_N^2
\end{aligned}
$$

The closer the variance is to zero, the more precise the estimate is to the Fourier reconstruction of the uncorrupted spectral data, $f_N(x)$. To reduce the variance, one can either decrease the total number of (pseudo-)spectral coefficients, or decrease the standard deviation of the correct spectral data. The value of the standard deviation of the correct spectral data is generally uncontrollable, and since high resolution reconstruction typically requires as many coefficients as possible, the variance cannot be reduced when the

standard Fourier reconstruction method is applied. The impact of noise can be seen in both the edge detection and Fourier reconstruction methods. Therefore, in order to improve the overall quality of the reconstructed image, the variance must be reduced in the edge detection procedure, and a different method must be utilized for reconstruction.

3.1. Reduction of Variance in Edge Detection

In order to reduce the variance of the edge detection method, we must first look at the impact that the corrupted Fourier coefficients (3.1) have on the expected value and variance of the concentration method (2.4). It is not difficult to show that

$$E\{T_N^\tau[f](x)\} = E\left\{i\pi \sum_{k=-N}^{N} \mathrm{sgn}(k)\, \tau\left(\frac{|k|}{N}\right)(\hat{f}_k + \hat{\xi}_k)\, e^{ik\pi x}\right\} = T_N^\tau[f](x)$$

which indicates that the average value of the concentration method is unaffected by noise. On the other hand, the variance of the concentration method,

$$\begin{aligned}
\mathrm{Var}(T_N^\tau[I](x)) &= E\left\{\left[i\pi \sum_{k=-N}^{N} \mathrm{sgn}(k)\, \tau\left(\frac{|k|}{N}\right)(\hat{f}_k + \hat{\xi}_k)\, e^{ik\pi x} - E\{T_N^\tau[f](x)\}\right]\right. \\
&\qquad \left.\cdot \left[i\pi \sum_{j=-N}^{N} \mathrm{sgn}(j)\, \tau\left(\frac{|j|}{N}\right)(\hat{f}_j + \hat{\xi}_j)\, e^{ij\pi x} - E\{T_N^\tau[f](x)\}\right]^*\right\}, \\
&= E\left\{\left[i\pi \sum_{k=-N}^{N} \mathrm{sgn}(k)\, \tau\left(\frac{|k|}{N}\right)\hat{\xi}_k e^{ik\pi x}\right]\right. \\
&\qquad \left.\cdot \left[i\pi \sum_{j=-N}^{N} \mathrm{sgn}(j)\, \tau\left(\frac{|j|}{N}\right)\hat{\xi}_j e^{ij\pi x}\right]^*\right\}, \\
&= \pi^2 \sum_{k=-N}^{N}\left(\mathrm{sgn}(k)\, \tau\left(\frac{|k|}{N}\right)\right)^2 \hat{\sigma}_{\hat{\xi}}^2 = \pi^2 \hat{\sigma}_{\hat{\xi}}^2 \sum_{k=-N}^{N} \tau\left(\frac{|k|}{N}\right)^2 \quad (3.3)
\end{aligned}$$

depends both on the variance of the noise, $\hat{\sigma}_{\hat{\xi}}^2$, as well as the concentration factor $\tau(\frac{|k|}{N})$. A careful choice of appropriate concentration factors will help to reduce the variance of the concentration method.

As is evident from the discussion in Section 2.1, the edge detection method, consisting of (2.4), (2.6), and (2.7), adequately resolves the locations of the jump discontinuities. However, in the presence of noise, the edge detection method might classify a point as a jump discontinuity that is really a continuous data point. Conversely, an edge may go undetected because it might appear as artificial noise in the image reconstruction. It is therefore useful to introduce another admissible concentration factor that
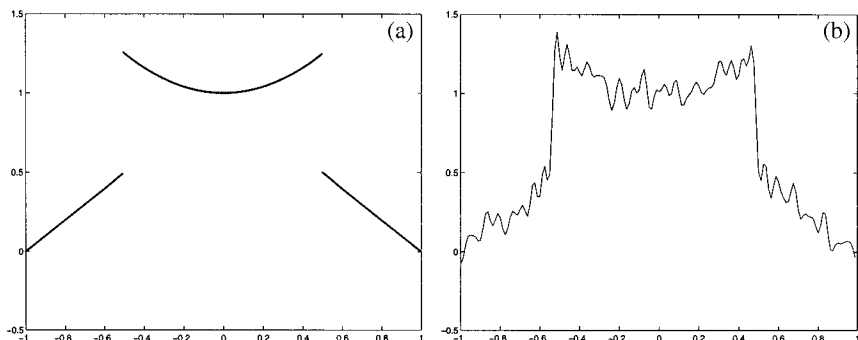
Fig. 2. (a) Example of a piecewise smooth function and (b) with noise added to the $N = 80$ Fourier coefficients by (3.1).

reduces the variance of the concentration method (3.3) in the presence of noise, given by

$$\sigma_n(\xi) = \text{Const} \cdot \xi e^{-\frac{\xi^2}{2\alpha^2}}, \qquad \tau_n(\xi) = \sigma_n(\xi) \frac{2 \sin\left(\dfrac{\xi\pi}{2}\right)}{\xi\pi} \qquad (3.4)$$

Here $\text{Const} = \frac{\sqrt{2}}{\alpha\sqrt{\pi}} - (1 - \Phi(\frac{1}{\alpha}))$ where Φ is the cumulative distribution function of a standard normal and $\alpha = 30$. In this case, τ_n represents an admissible concentration factor that better captures the jump discontinuities in the presence of noise, basically by extracting out the high frequency Fourier coefficients. This Gaussian smoothing concentration factor can be used as a secondary test to ensure that the jump discontinuities are correctly identified by the concentration method. In fact, the possibility of the occurence of both types of misidentification discussed above is reduced by applying the concentration method twice, first with a concentration factor such as τ_e (2.5), and then by using τ_n.

To demonstrate the effects of noise on edge detection and the reduction of error by applying the concentration method in this way, consider the example displayed in Fig. 2. The effects of noise causes the misidentification of a jump discontinuity, as exhibited in Fig. 3(a). After evaluating the edges with τ_e (2.5), it appears that there are three discontinuities. But the second application of the edge detection method on these identified points using τ_n (3.4), depicted in Fig. 3(b), greatly reduces the size of the misclassified jump discontinuity. As a result, one would conclude that this point is not a true jump discontinuity of the function. The possibility of edges going undetected in the presence of noise due to the interference of the scaling of the noise with the small scale of the jump discontinuities is similarly handled [1].
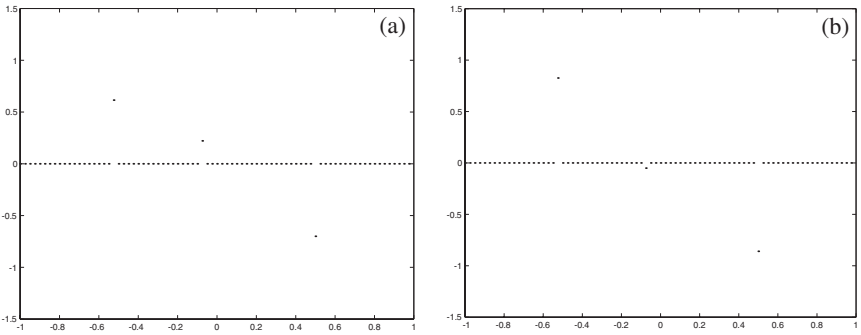
Fig. 3. Edge detection applied to the example in figure using the concentration factor given by (a) τ_e and (b) τ_n.

4. REDUCTION OF VARIANCE IN RECONSTRUCTION

In order to reduce the variance for image reconstruction, we must first look at how the corrupted spectral data (3.1) impacts reconstruction. Since the variance cannot be further reduced in the standard Fourier reconstruction method, let us instead consider the filtered Fourier reconstruction,

$$f_N^\theta(x) = \sum_{k=-N}^{N} \theta_k \hat{f}_k e^{ik\pi x}$$

where θ_k denotes a standard filter, for example the exponential filter, $\theta_k = e^{-\alpha\left(\frac{|k|}{N}\right)^p}$. The expectation of the filtered Fourier reconstruction of the image,

$$E\{I_N^\theta(x)\} = E\left\{ \sum_{k=-N}^{N} \theta_k (\hat{f}_k + \hat{\xi}_k)\, e^{ik\pi x} \right\} = f_N^\theta(x)$$

is simply the result of the filtered Fourier reconstruction, implying that the filtered Fourier reconstruction method is an unbiased estimator. The variance is calculated as

$$\begin{aligned}
\mathrm{Var}(I_N^\theta(x)) &= E\left\{ \left[\sum_{k=-N}^{N} \theta_k (\hat{f}_k + \hat{\xi}_k)\, e^{ik\pi x} - E\{I_N^\theta(x)\} \right] \right. \\
&\quad \left. \cdot \left[\sum_{j=-N}^{N} \theta_j (\hat{f}_j + \hat{\xi}_j)\, e^{ij\pi x} - E\{I_N^\theta(x)\} \right]^* \right\}, \\
&= E\left\{ \left[\sum_{k=-N}^{N} \theta_k \hat{\xi}_k e^{ik\pi x} \right] \cdot \left[\sum_{j=-N}^{N} \theta_j \hat{\xi}_j e^{ij\pi x} \right]^* \right\} = \sum_{k=-N}^{N} \theta_k^2 \hat{\sigma}_{\hat{\xi}}^2, \\
&= \hat{\sigma}_{\hat{\xi}}^2 \sum_{k=-N}^{N} \theta_k^2 = \hat{\sigma}_{\hat{\xi}}^2 \bar{\Theta}(N, \alpha, p)
\end{aligned}$$

suggesting that it is indeed possible to reduce the variance by filtering.

The Gegenbauer reconstruction method is another possible way to reduce variance in the presence of noise. The expectation is computed as

$$E\{g_m^\lambda(I_N(x(\eta)))\} = E\left\{\sum_{l=0}^m \frac{1}{h_l^\lambda}\left(\int_{-1}^1 (1-\eta^2)^{\lambda-\frac{1}{2}} C_l^\lambda(\eta)\, f_N(x(\eta))\, d\eta\right.\right.$$
$$\left.\left. + \int_{-1}^1 (1-\eta^2)^{\lambda-\frac{1}{2}} C_l^\lambda(\eta)\, \xi_N(x(\eta))\, d\eta\right) C_l^\lambda(\eta)\right\},$$
$$= \sum_{l=0}^m \hat{g}_{l,\epsilon}^\lambda\, C_l^\lambda(\eta) = g_m^\lambda(x(\eta))$$

Thus the Gegenbauer method is also an unbiased estimator. If we define

$$\hat{\xi}_l^\lambda = \int_{-1}^1 (1-\eta^2)^{\lambda-\frac{1}{2}} C_l^\lambda(\eta)\, \xi_N(x(\eta))\, d\eta$$

then the variance is given as

$$\mathrm{Var}(g^\lambda(I_N(x(\eta))) = E\{[g_m^\lambda(I_N(x(\eta)))-E\{g_m^\lambda(I_N(x(\eta)))\}]$$
$$\cdot [g_m^\lambda(I_N(x(\eta)))-E\{g_m^\lambda(I_N(x(\eta)))\}]^*\},$$
$$= E\left\{\left[\sum_{k=0}^m \hat{\xi}_k^\lambda C_k^\lambda(\eta)\right]\cdot\left[\sum_{l=0}^m \hat{\xi}_l^\lambda C_l^\lambda(\eta)\right]^*\right\},$$
$$= \sum_{k=0}^m \sum_{l=0}^m E\{\hat{\xi}_k^\lambda \cdot [\hat{\xi}_l^\lambda]^*\}\, C_k^\lambda(\eta)\, C_l^\lambda(\eta),$$
$$= \hat{\sigma}_{\hat{\xi}}^2 \sum_{k=0}^m \sum_{l=0}^m \left(\delta_{0k}\delta_{0l} + \Gamma^2(\lambda)\, i^{k-l}(k+\lambda)(l+\lambda)\right.$$
$$\left. \times \sum_{0<|j|\leq N} J_{k+\lambda}(\pi j\epsilon)\left(\frac{2}{\pi j\epsilon}\right)^{2\lambda} J_{l+\lambda}(\pi j\epsilon)\, e^{2ij\pi\delta}\right) C_k^\lambda(\eta)\, C_l^\lambda(\eta).$$
$$= \hat{\sigma}_{\hat{\xi}}^2 \bar{G}(\eta, m, \lambda, N)$$

Hence the variance depends on the particular approximation location, $x(\eta)$. Figure 4 compares the results of the filtered Fourier and Gegenbauer reconstruction methods for the example in Fig. 2 when random noise is added to the coefficients. As depicted in Figs. 4(a), 4(b), and 5(a), the Gegenbauer reconstruction method is more effective at reducing the overall error. Yet it is clear in Fig. 5(b) that the variance for the Gegenbauer reconstruction method is not reduced near $\eta = \pm 1$. This discrepancy will be the topic of future papers. Clearly heavier filtering and lower order Gegenbauer polynomial reconstruction will reduce the variance, but only by allowing undesirable smoothing of the finer features of the function.
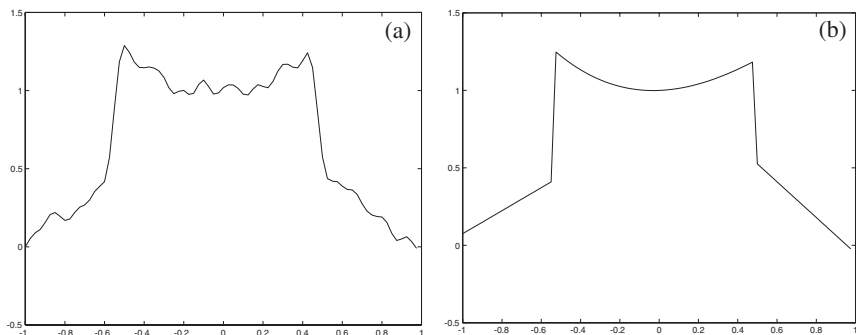
Fig. 4. Reconstruction of the example in figure using (a) filtered Fourier ($p = 4$, $\alpha = 16$) and (b) Gegenbauer methods ($m = \lambda = 4$).
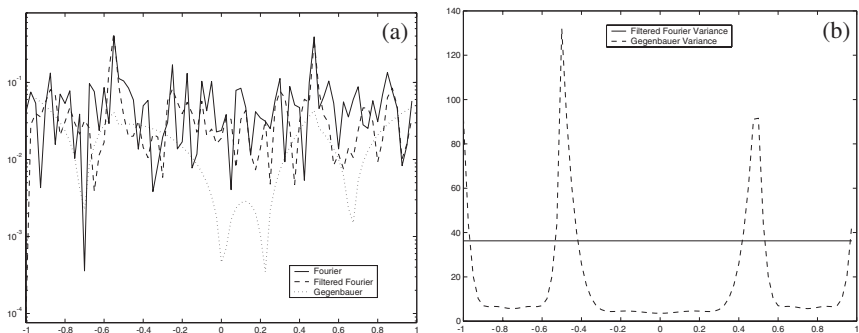
Fig. 5. (a) Logarithmic error in the reconstruction of the example in figure using Fourier, filtered Fourier of order 4, and Gegenbauer reconstruction ($m = \lambda = 4$) techniques when noise is added to the Fourier coefficients. (b) Comparison of $\bar{G}(\eta, m, \lambda, N)$ and $\bar{\Theta}(N, \alpha, p)$.
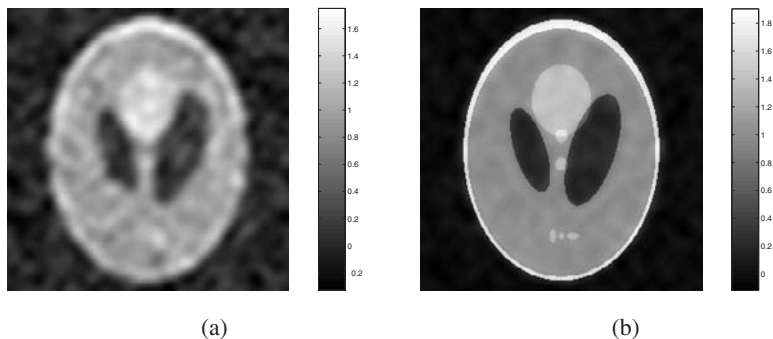
Fig. 6. Reconstruction of the Shepp Logan phantom in the presence of noise using (a) filtered Fourier with $p = 4$ and (b) Gegenbauer with $m = \lambda \approx \frac{\epsilon N}{8}$ reconstruction techniques.

To conclude this section, we once again return to the example of the Shepp Logan brain phantom to illustrate the efficacy of the edge detection procedure and Gegenbauer reconstruction method in the presence of noise. As shown in Fig. 6(a), the effects of noise to the Shepp Logan image is reduced by applying a standard exponential filter, but only at the cost of blurring near the edges. The image reconstruction is greatly improved when applying the Gegenbauer reconstruction method, as seen in 6(b).

5. CONCLUDING REMARKS

In this paper we demonstrated how the edge detection and Gegenbauer reconstruction methods are not only effective for reconstructing piecewise smooth functions from Fourier spectral data, but they are also robust in the presence of noise. Specifically, the edge detection method can be modified to consider data contaminated by random noise. Although the reduction of the variance of reconstruction by the Gegenbauer method is difficult to quantify, numerical evidence strongly supports that this is the case. We note that the edge detection and Gegenbauer reconstruction methods both take advantage of the FFT algorithms, making the method computationally comparable to standard imaging techniques for rectilinear coordinates [12]. However, computational efficiency of the minimization problem (2.7) must be further addressed, as well as manipulation of the Gegenbauer reconstruction method to reduce the variance of the reconstructed image. These will be topics of future work.

ACKNOWLEDGMENTS

REFERENCES

1. Archibald, R., *New Numerical Techniques for Segmentation and Reconstruction of Medical Images*, Ph.D. thesis, Arizona State University. In progress.
2. Archibald, R., and Gelb, A. (2001). A method to reduce the Gibbs ringing artifact in MRI scans while keeping tissue boundary integrity. Submitted to *IEEE Trans. Med. Imaging*.
3. Bateman, H. (1953). *Higher Transcendental Functions*, Vol. 2, McGraw-Hill, New York.
4. Cai, W., Gottlieb, D., and Shu, C.-W. (1989). Essentially non-oscillatory spectral Fourier methods for shock wave calculations. *Math. Comp.* **52**, 389–410.
5. Eckhoff, K. S. (1995). Accurate reconstructions of functions of finite regularity from truncated series expansions. *Math. Comp.* **64**, 671–690.
6. Eckhoff, K. S. (1998). On a high order numerical method for functions with singularities. *Math. Comp.* **67**, 1063–1087.
7. Gelb, A., and Tadmor, E. (1999). Detection of edges in spectral data. *Appl. Comput. Harmon. Anal.* **7**, 101–135.

8. Gelb, A., and Tadmor, E. (2000). Detection of edges in spectral data II. Nonlinear enhancement. *SIAM J. Numer. Anal.* **38**, 1389–1408.

9. Gottlieb, D., Gustafsson, B., and Forssen, P. (2000). On the direct Fourier method for computer tomography. *IEEE Transactions of Medical Imaging* **19**, 223–233.

10. Gottlieb D., and Shu, C.-W. (1997). On the Gibbs phenomenon and its resolution. *SIAM Review*.

11. Gottlieb, D., Shu, C.-W., Solomonoff, A., and Vandeven, H. (1992). On the Gibbs phenomenon I: Recovering exponential accuracy from the Fourier partial sum of a non-periodic analytic function. *J. Comput. Appl. Math.* **43**, 81–92.

12. Liang, Z. P., and Lauterbur, P. (2000). *Principles of Magnetic Resonance Imaging*, IEEE Press.